AIAA JOURNAL
Vol. 39, No. 12, December 2001

Chemistry of JP-10 Ignition

S. C. Li,* B. Varatharajan,† and F. A. Williams‡
University of California, San Diego, La Jolla, California 92093-0411

Ignition of JP-10 is addressed from computational and theoretical viewpoints. A detailed chemical mechanism consisting of 174 elementary steps among 36 chemical species is obtained by adding 27 steps, including JP-10, cyclopentene, and 1,3 butadiene, to an earlier system of 147 steps among 33 species that extend through C_3 hydrocarbons. The new steps and their rate parameters are derived by analogy with earlier studies of decane and heptane. Predictions of ignition times by the new detailed mechanism are found to be in good agreement with data from JP-10 shock-tube experiments. Systematically reduced mechanisms also are discussed on the basis of the detailed mechanism, resulting in a simplified correlation that performs well. The results can be helpful for applications in airbreathing propulsion involving JP-10.

Introduction

THE single-component hydrocarbon JP-10 ($C_{10}H_{16}$, tricyclo [5.2.1.0^{2,6}] decane) is synthetically produced by hydrogenation of dicyclopentadiene and is used in volume-limited combustion chambers such as those of supersonic-combustion ramjets and pulse-detonation engines. To help understand how JP-10 ignition occurs in these combustors, the present study addresses reaction mechanisms with the objective of predicting autoignition times for temperatures between 1000 and 2500 K, pressures between 1 and 100 bar, and equivalence ratios between 0.5 and 2.0, the range of conditions considered most appropriate to these propulsion applications. The research continues investigations of higher hydrocarbon flame chemistry[1] and refines earlier JP-10 ignition work.[2]

Unlike most practical fuels, JP-10 is not a mixture and, therefore, is more readily amenable to theoretical modeling. It is, however, too large a molecule for complete detailed descriptions of its decomposition and combustion chemistry to be developed, descriptions of the types that have been successful for methane, ethane, and other lower hydrocarbons. Instead, in the fuel chemistry of JP-10, overall approximations are needed for effects of sequences of elementary reaction steps, approximations of the kinds that have been employed, for example, for heptane.[3] Resulting theoretical predictions, therefore, need to be tested carefully against experimental data. Although burning and evaporation rates of JP-10 droplets have been measured[4] and its wide use in slurry-fuel applications has led to a number of experiments on its slurry-droplet combustion behavior,[5,6] there are relatively few measurements of its ignition delay times, data that are needed for applications to high-speed propulsion. Some measurements of JP-10 have been made for liquid fuel injected into a heated cylindrical bomb,[7] but cleaner shock-tube ignition-delay experiments are desirable for finer testing. Although the comparatively low vapor pressure of JP-10 complicates such experiments, useful shock-tube results have been obtained recently.[8,9] Comparisons are made with these recent data in the present paper.

Chemical Mechanism

The new mechanism introduced here consists of 174 reactions among the 36 species, O_2, H_2, H_2O, HO_2, H_2O_2, H, OH, O, CO, CO_2, CH_4, CH_3, CH_3O, CH_2OH, CH_2O, CHO, singlet CH_2 and triplet CH_2, CH, C_2H, HCCO, CH_2CO, CH_2CHO, C_2H_2, C_2H_3, C_2H_4, C_2H_5, C_2H_6, C_3H_3, C_3H_4, C_3H_5, C_3H_6, C_3H_7, C_4H_6, C_5H_8, and JP-10. The first part of the mechanism is the chemistry of JP-10 breakdown to form smaller hydrocarbons that contain no more than three carbon atoms (C_1–C_3 species), given in Table 1, whereas the rest of the mechanism consists of our previous detailed chemical reaction mechanisms for C_1–C_3 species. The C_1–C_3 reaction mechanism,[10] consisting of 147 elementary reactions among the first 33 species just listed, has been tested for ignition and combustion of methane,[11,12] methanol,[13] acetylene,[14,15] ethylene,[10] and ethane,[16] and the rate parameters of all of its 147 elementary reactions are employed here without change.

In view of the earlier publications, nothing more needs to be said about the C_1–C_3 chemistry. The new steps that have been added for addressing JP-10, however, require further discussion. Two different types of initiation steps need to be considered. One is the nonoxidative pyrolytic decomposition of JP-10, and the other its oxidative pyrolysis. Although there appears to be no experimental information on oxidative pyrolysis, preliminary studies of nonoxidative pyrolysis have been made,[17] suggesting that proton attack produces C_7, C_6, and C_5 species, whereas thermal pyrolysis around 1000 K may yield benzene. Our proposed mechanism involves three unimolecular overall decomposition steps, two of which include a C_5 species (cyclopentene), namely, decomposition to $H + C_2H_4 + C_3H_3 + C_5H_8$ and to $H + C_2H_2 + C_3H_5 + C_5H_8$; the other, the first reaction in Table 1, yields $C_2H_2 + 2C_2H_4 + C_4H_6$ (1,3 butadiene). Overall rate parameters were assigned by analogy with what has been done previously for normal alkanes.[3,18,19] With these parameters, the last step just mentioned appears to be more important than the other two, and above about 1500 K it even begins to dominate the overall effects of oxidative pyrolysis.

The selection of these three overall decomposition steps and of their rates is based on considerations of the structure of the JP-10 molecule. The two steps identified initially (the second and third in Table 1) begin with rupture of a C–H bond of a CH_2 group and are assigned an activation energy comparable with that bond energy and a prefactor comparable with those for breaking corresponding C–H bonds in C_{10} alkanes. The rupture is then assumed to be followed by four C–C bond scissions that break two of the five-member rings and leave one cyclopentene group intact. The location of the initial bond rupture and the sequence of subsequent scissions then lead to one or the other of the first two sets of products given.

Note at the outset that these decomposition steps are highly speculative, as are many of the other steps in Table 1. The selection here is only a first try, and the results are inconsistent with much of the currently emerging evidence about product distributions, such as the aforementioned likely observation of production of benzene.

Received 30 January 2001; revision received 20 April 2001; accepted for publication 30 April 2001.

*Research Scientist, Center for Energy Research, Department of Mechanical and Aerospace Engineering, 9500 Gilman Drive.

†Graduate Student, Center for Energy Research, Department of Mechanical and Aerospace Engineering; currently Mechanical Engineer, Engineering Systems Laboratory, General Electric Co., Building K-1, Room ES-612B, P.O. Box 8, Schenectady, NY 12301; varathar@crd.ge.com. Student Member AIAA.

‡Professor and Director, Center for Energy Research, Department of Mechanical and Aerospace Engineering, 9500 Gilman Drive. Fellow AIAA.

Table 1 New irreversible reaction steps and associate rate parameters employed in describing ignition and combustion of JP-10; specific reaction-rate constant $k = AT^n \exp(-E/RT)$

Number	Reaction	A^a	n^a	E^a
1	$C_{10}H_{16} \rightarrow C_2H_2 + 2\,C_2H_4 + C_4H_6$	5.00×10^{16}	0.0	85.4
2	$C_{10}H_{16} \rightarrow H + C_2H_4 + C_3H_3 + C_5H_8$	6.00×10^{16}	0.0	98.0
3	$C_{10}H_{16} \rightarrow H + C_2H_2 + C_3H_5 + C_5H_8$	6.00×10^{16}	0.0	98.0
4	$C_{10}H_{16} + O_2 \rightarrow HO_2 + C_2H_4 + C_3H_3 + C_5H_8$	3.98×10^{13}	0.0	50.9
5	$C_{10}H_{16} + O_2 \rightarrow HO_2 + C_2H_2 + C_3H_5 + C_5H_8$	7.92×10^{13}	0.0	47.6
6	$C_{10}H_{16} + OH \rightarrow H_2O + C_2H_4 + C_3H_3 + C_5H_8$	1.74×10^{7}	1.8	1.0
7	$C_{10}H_{16} + OH \rightarrow H_2O + C_2H_2 + C_3H_5 + C_5H_8$	3.80×10^{6}	2.0	−0.6
8	$C_{10}H_{16} + O \rightarrow OH + C_2H_4 + C_3H_3 + C_5H_8$	2.88×10^{6}	2.4	5.5
9	$C_{10}H_{16} + O \rightarrow OH + C_2H_2 + C_3H_5 + C_5H_8$	2.76×10^{5}	2.6	1.9
10	$C_{10}H_{16} + H \rightarrow H_2 + C_2H_4 + C_3H_3 + C_5H_8$	1.32×10^{6}	2.5	6.8
11	$C_{10}H_{16} + H \rightarrow H_2 + C_2H_2 + C_3H_5 + C_5H_8$	2.60×10^{6}	2.4	4.5
12	$C_{10}H_{16} + HO_2 \rightarrow H_2O_2 + C_2H_4 + C_3H_3 + C_5H_8$	4.76×10^{4}	2.5	16.5
13	$C_{10}H_{16} + HO_2 \rightarrow H_2O_2 + C_2H_2 + C_3H_5 + C_5H_8$	1.93×10^{4}	2.6	13.9
14	$C_5H_8 \rightarrow C_2H_4 + C_3H_4$	3.16×10^{12}	0.0	57.0
15	$C_5H_8 \rightarrow C_2H_3 + C_3H_5$	3.16×10^{12}	0.0	57.0
16	$C_5H_8 \rightarrow C_2H_2 + C_3H_6$	1.00×10^{16}	0.0	73.0
17	$C_5H_8 + O_2 \rightarrow HO_2 + C_2H_2 + C_3H_5$	3.00×10^{12}	0.0	0.0
18	$C_5H_8 + O_2 \rightarrow HO_2 + C_2H_3 + C_3H_4$	3.00×10^{12}	0.0	0.0
19	$C_5H_8 + HO_2 \rightarrow H_2O_2 + C_2H_2 + C_3H_5$	1.00×10^{14}	0.0	0.0
20	$C_5H_8 + HO_2 \rightarrow H_2O_2 + C_2H_3 + C_3H_4$	1.00×10^{14}	0.0	0.0
21	$C_4H_6 \rightarrow 2C_2H_3$	1.80×10^{13}	0.0	85.1
22	$2C_2H_3 \rightarrow C_4H_6$	1.26×10^{13}	0.0	0.0
23	$C_3H_3 + CH_3 \rightarrow C_4H_6$	5.00×10^{12}	0.0	0.0
24	$C_4H_6 \rightarrow H + C_2H_2 + C_2H_3$	1.58×10^{16}	0.0	109.9
25	$C_4H_6 + OH \rightarrow CHO + H + C_3H_5$	5.00×10^{12}	0.0	0.0
26	$C_4H_6 + H \rightarrow H_2 + C_2H_2 + C_2H_3$	6.30×10^{10}	0.7	6.0
27	$C_4H_6 + H \rightarrow C_2H_3 + C_2H_4$	5.00×10^{11}	0.0	0.0
28	$C_4H_6 + CH_3 \rightarrow CH_4 + C_2H_2 + C_2H_3$	7.00×10^{13}	0.0	18.4

[a] Units: mol, cm^3, s, K, and kcal/mol.

The objective is to obtain a short mechanism that arrives as quickly as possible at species containing no more than three carbon atoms, where the chemistry reaches firmer ground. To accomplish this, C_6 species, for example, are not addressed, the largest initial products admitted being C_5. Readers should be strongly cautioned to refrain from using the current mechanism to predict product distributions above C_3, to predict results for equivalence ratios above 2.0, or to make predictions for temperatures below 1000 K. Even within the range of the present application, the mechanism almost certainly is wrong in detail. Correct mechanisms are likely to include benzene and cyclopentadiene, for example, and they also are likely to be much larger than the present mechanism. It is possible that such correct mechanisms can be reduced systematically to mechanisms of the present brevity. A proper complete study, which would be worthwhile, would, however, be very ambitious and time consuming, and the final results at the C_3 level and lower may not differ much from the present results. It is, thus, with the intent of obtaining potentially useable results with reasonable expediency that the present work was performed.

To further illustrate the character of the level of the present description, it is of interest to address the first entry in Table 1 in greater detail. The set of products in the first step of Table 1 is formed as illustrated in Fig. 1. In Fig. 1, the seven different kinds of C–C bonds in the JP-10 molecule are numbered from 1 to 7 for purposes of discussion. It is assumed that the unique bond 5, the only bond between two CH groups that is common to two five-member rings, breaks first, and the rate is assigned an activation energy comparable to the C–C bond energy and a prefactor comparable with those for C–C bond breaking in C_{10} alkanes. Two β scissions are then assumed to break C–C bonds of types 7 and 6, in that order, yielding ethylene and the radical shown next in Fig. 1. A further β scission then can give the isooctadiene biradical shown next in Fig. 1, which may form acetylene and the isohexadiene biradical shown last, the latter readily yielding C_2H_4 and 1,3-C_4H_6.

Although the conceptual sequence just described represents only one of many possibilities, it helps to motivate the hypothesized product distribution in this selected overall pyrolysis step. It moreover illustrates the degree of approximation involved in the level of description that is adopted for the detailed mechanism in the present work. Further study definitely is needed of the detailed JP-10 pyrolysis mechanism, as was indicated. The simple β-scission sequences adopted here, patterned after alkanes, in fact may not be very relevant to JP-10. Cyclo compounds and olefins, for example, are known to decompose often by other mechanisms, such as concerted retroene processes having lower activation energies, and these could be especially dominant at the lowest temperatures of interest here. Although much relevant information is available,[20] the JP-10 problem is more

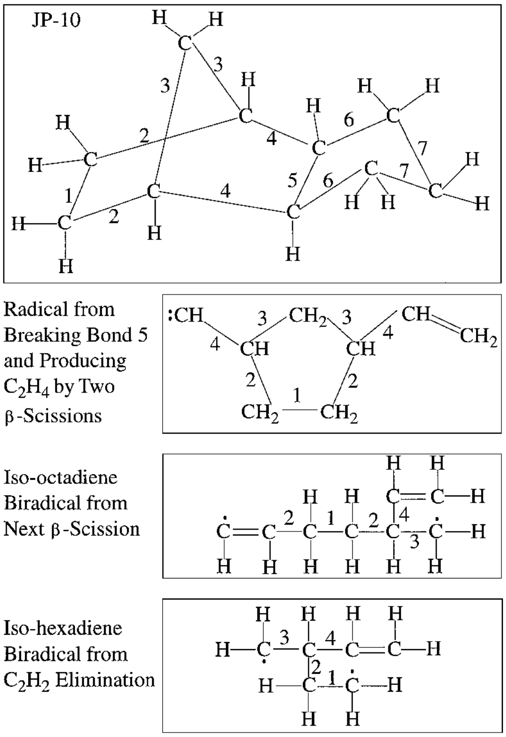

Fig. 1 Mechanism of breakdown of JP-10 to form the set of products listed in step 1 of Table 1.

complicated and unsolved. Future investigations, which might produce results in reasonable agreement with the present results in some respects for different reasons, would necessarily involve a more complex mechanism that would be more time-consuming computationally, at least before reduction. The performance of the present degree of approximation, therefore, seems worth exploring.

As is usually found in these ignition and combustion problems, oxidative pyrolysis plays a greater role than the preceding decompositions under many conditions. Two such oxidative steps were included, again with rate parameters obtained by analogy with heptane[3] and decane,[18] namely, steps to the products $HO_2 + C_2H_4 + C_3H_3 + C_5H_8$ and $HO_2 + C_2H_2 + C_3H_5 + C_5H_8$, the latter roughly twice as fast as the former. They begin with H abstraction and proceed through the same β-scission sequence that was indicated earlier to follow C–H bond rapture. These two steps, reactions 4 and 5 in Table 1, were found to be the principal overall initiation steps with the selected mechanism. Their inclusion yields results differing from those of our earliest preliminary work, in which only nonoxidative pyrolysis was employed.

Following initiation, radical attack on the parent molecule plays a very important part in the continuing high-temperature fuel chemistry. These steps, too, were absent in our earliest preliminary work. Similar to the initiation steps, they require overall modeling.[3] With the rate parameters selected, the most important steps were found to be OH attack to form $H_2O + C_2H_4 + C_3H_3 + C_5H_8$ and $H_2O + C_2H_2 + C_3H_5 + C_5H_8$; O attack to form OH along with these same two sets of hydrocarbon fragments; and, similarly, H attack to form H_2 plus the fragments. In all cases, then, hydrogen abstraction initiates internal β scissions that result in the C_2 species and C_3 species, leaving behind the five-member ring. This breakdown is the same as the result of H abstraction by O_2 in the oxidative initiation step and the C–H bond rupture in the nonoxidative pyrolysis. Similar to the O_2 attack, the abstraction by H favors acetylene over ethylene by slightly more than a two-to-one margin, but the OH and O attacks in this description favor ethylene much more strongly, causing C_2H_4 to play a more dominant role in the subsequent chemistry. Its increased rate of direct formation at high temperatures through the first step of Table 1, in fact, diminishes the importance of radical attack on $C_{10}H_{16}$ at high temperatures. The radical attacks that were included are steps 6–13 in Table 1, the last two found to be of lesser importance with the rate parameters selected.

The adopted mechanism has seven steps for removal of the C_5H_8 produced in the preceding mechanisms, steps 14–20 in Table 1, with rates estimated from 1-pentene values of Held et al.[3] and other literature. Three are direct nonoxidative decompositions that probably are not elementary steps, even though they appear that they could be, and the other four involve H-atom abstraction by O_2 or HO_2 and are more clearly overall approximations, their selected rates being high enough that it was unnecessary to include attacks by OH, O, or H. The most important were found to be the two abstractions by O_2. Eight steps involving 1,3 butadiene also are included, steps 21–28 in Table 1, with rate parameters taken from Held et al.,[3] the most important being OH and H attack to form $CHO + H + C_3H_5$ and $H_2 + C_2H_2 + C_2H_3$, respectively. All new steps are irreversible, consistent with the overall chemistry approximation, although the reverse of one of the C_4H_6 steps (step 21) is included, (step 22, numbered separately in Table 1, with a reliable rate parameter from a different source, inconsistent with the equilibrium constant). Table 1 thus lists all new steps and associated rate parameters that were added to our earlier set specfically for addressing JP-10 ignition and combustion. Specific choices of rate parameters for most steps 14–28 have little effect on calculated ignition times, so that the rough approximations introduced for some of these steps are not critical.

Comparisons of Predictions with Shock-Tube Induction Times

Figure 2 compares measured[8,9] ignition delays with predictions of numerical computations employing the present mechanism. The numerical code used was FlameMaster.[21] The dashed line in each panel of Fig. 2, discussed in the following section, is a correlation of the form

$$\tau = 1.26 \times 10^{-17} [O_2]^{-1} e^{23,970/T} \qquad (1)$$

with τ the ignition time in seconds, $[O_2]$ the oxygen concentration in mole per cubic centimeter and T the temperature in degrees Kelvin. This correlation is similar to one given by Colket and Spadaccini[8] but has different powers of concentration. The computed ignition delay is defined as the time of maximum rate of increase of temperature, which should coincide closely with the maximum rate of increase of pressure in the shock-tube experiments. The measurements were made behind the reflected shock, with ignition times defined by a large rate of increase of OH emission intensity[8] or by a maximum CH emission intensity,[9] both reasoned[8,9] to correspond closely with the maximum rate of pressure increase. It is, therefore, appropriate to compare the predictions with these experiments. The agreement between experiment and prediction is seen to be typically better than within a factor of two, although the predicted overall activation energy seems slightly larger over the range of the data and the predicted ignition time systematically low at the leanest condition.

These comparisons indicate that, although agreements are acceptable for many purposes, it is desirable to devote further study to the detailed chemistry of JP-10 ignition. There are two appropriate directions for this further work. One is to improve the fuel chemistry discussed in the preceding section, testing and improving the rate parameters for the overall steps listed in Table 1, as well as deriving more detailed chemical–kinetic descriptions that involve lesser degrees of overall step approximations. The other direction is to reduce the chemistry further so that shorter overall mechanisms are obtained that can be applied more readily in a variety of different propulsion calculations. It is of interest to discuss briefly ways in which further simplifications of the latter type may be obtained.

Reduced Chemistry

Steady-state approximations have been found to be reasonable for various intermediate species during ignition processes. Introduction of steady states has the effect of decreasing the number of steps in the overall mechanism. Use has been made of steady-state approximations to reduce the chemistry for ignition of methane,[12] acetylene,[14] and ethylene.[10] The character of the resulting simplified chemistry differs among these three fuels. For methane, there is a nonlinear chain-branching stage that exhibits a branched-chain thermal-explosion character.[12] Acetylene, on the other hand, exhibits a linear chain-branching stage with a branched-chain thermal-explosion character.[14] For that fuel, it was possible to introduce simplifying approximations that ultimately resulted in a one-step description of the ignition chemistry.[14] Ethylene, too, exhibited a linear chain-branching stage, but for this fuel fewer steady-state approximations applied, and identities of steady-state species varied appreciably with temperature.[10] The effective overall activation energy for ignition, thus, depended more on the variation of the mechanism with temperature than on activation energies of individual steps, necessitating a more empirical approach to achieving simplification. An additional complication for ethylene at the lower temperatures is the occurrence of an identifiable stage of nearly constant composition after chain branching, with thermal runaway in this stage replacing the branched-chain thermal explosion.[10] Because of the significant amount of ethylene produced in the JP-10 ignition process, these aspects of ethylene ignition may be expected to be reflected to some extent in JP-10 ignition, thereby necessitating more empirical approaches to achieving significant simplifications.

The extent to which ignition of JP-10 parallels ignition of these simpler molecules can be discussed on the basis of histories of species concentrations and temperature, computed from the detailed mechanism. Figure 3 shows results of such a calculation for one representative condition. Although the calculation was made for an isobaric adiabatic system, at least up until ignition, the results are essentially the same as those for an isochoric adiabatic system, selected more often in modeling shock-tube ignition. The general characteristics exhibited in Fig. 3 were found to extend over the entire range of conditions addressed here, so that it is unnecessary to show results for other conditions. The main conclusion to be drawn from Fig. 3 is that JP-10 ignition differs qualitatively from ignition of all of the simpler fuels described earlier, as will now be discussed.

From the temperature history in Fig. 3, it is seen that there is an initial endothermic period during which the temperature decreases.

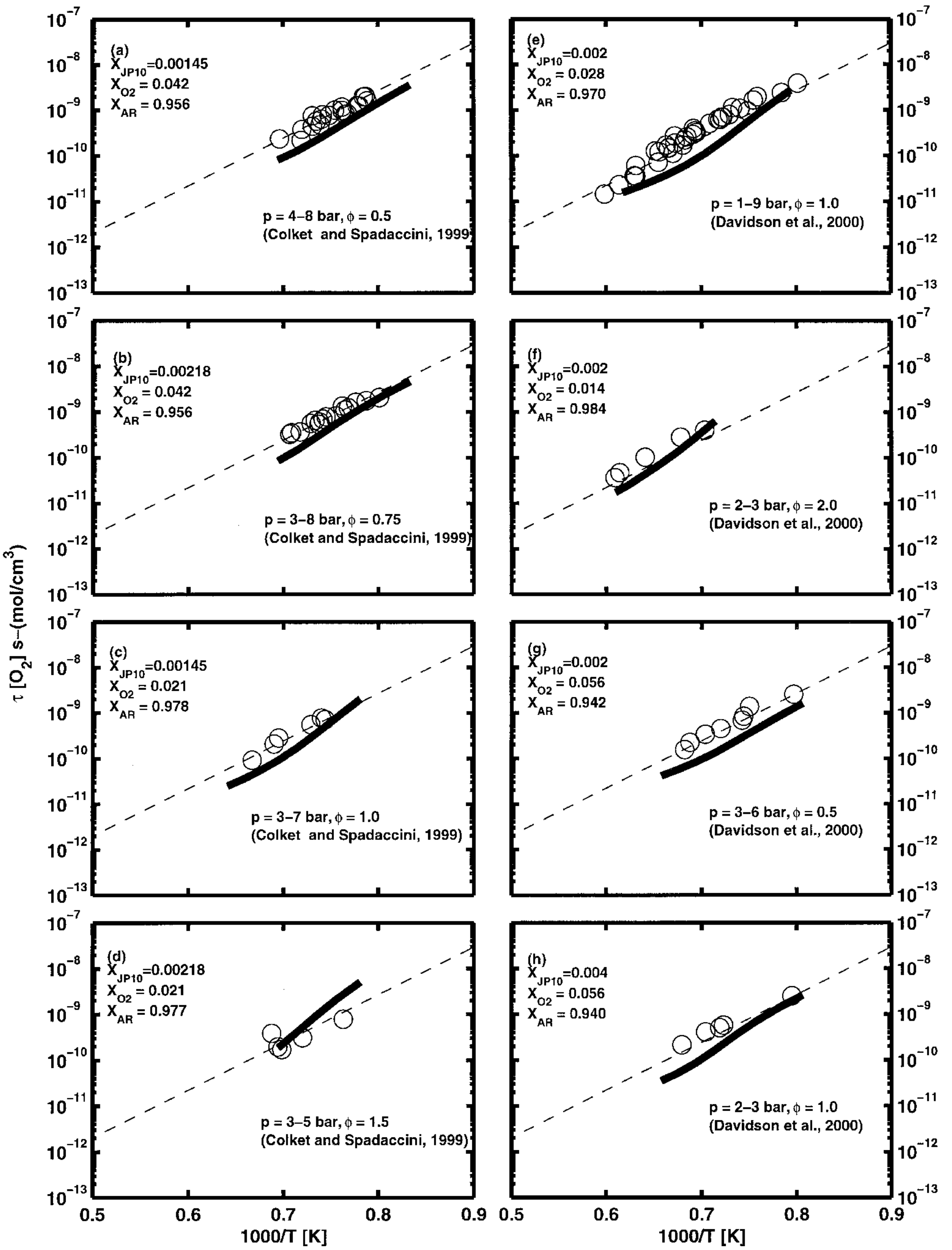

Fig. 2 Comparison of measured ignition times with those predicted by detailed mechanism (——) and by simplified correlation (- - -); *p* denotes pressure, ϕ equivalence ratio, and *X* mole fraction.

The extent of the decrease increases with increasing initial temperature and is quite pronounced at initial temperatures of 2000 K and above. Such temperature dips are not seen at all for most lighter fuels and are much shallower for the few lighter fuels for which they are observed. Noticeable initial temperature decreases in autoignition are found for heavier fuels, such as heptane, but even for these fuels they are not as strong as for JP-10. This behavior is consistent with the reputation of JP-10 as an endothermic fuel, that is, as a fuel with increased effectiveness as a coolant, and it is associated with the stability of the fuel molecule, reflected in the relatively large endothermicity of its initial stages of breakdown. Although this endothermicity contributes to the relatively long ignition time of JP-10, it does not appear to be the dominant factor, as explained hereafter.

The $C_{10}H_{16}$ concentration is seen in Fig. 3 to decrease fairly rapidly initially, resulting in rapid buildup of concentrations of mainly C_2H_4 and C_2H_2. Concentrations of these two species quickly level off, nearly approaching values that would occur if all of the parent fuel were to decompose completely to these C_2 species, and these near-maximum values are maintained approximately constant for most of the ignition delay period. Although the high concentrations of these C_2 species argue for their relevance in JP-10 ignition, the ignition mechanism appears to be quite different from that of either C_2H_2 or C_2H_4. The reason is the continuing role played by $C_{10}H_{16}$ in the induction process. Figure 3 shows that the $C_{10}H_{16}$ concentration continues to decrease during ignition and that the radical concentrations and temperature begin to increase rapidly only after the $C_{10}H_{16}$ concentration has fallen below the radical concentrations. Essentially, the parent fuel is a strong sink for radicals, so that appreciable branching and thermal runaway can begin only after the $C_{10}H_{16}$ concentration becomes negligible in comparison with concentrations of major radicals such as OH and H. It can be inferred that the affinity of $C_{10}H_{16}$ for radicals is so strong that, after the initial radical buildup, it causes the concentrations of OH, H, O, and C_2H_3 actually to decrease with time for a short period early during induction, just after initiation, as seen in Fig. 3.

The strong radical-scavenging effect of $C_{10}H_{16}$ can be understood from the steps in Table 1. If, for simplicity, steady states are hypothesized for C_5H_8, C_4H_6, C_3H_5, C_3H_4, C_3H_3, and CHO, and

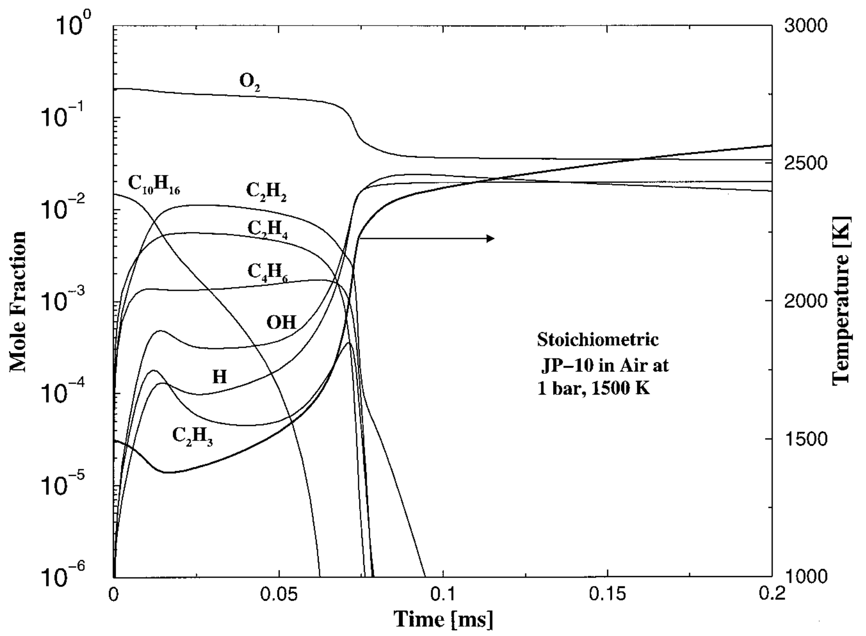

Fig. 3 Predicted histories of species concentrations and of temperature for autoignition of stoichiometric mixture of JP-10 in air at 1 bar and initial temperature of 1500 K.

steps 14 and 25 of Table 1, along with $C_3H_5 + H \rightarrow C_3H_4 + H_2$, $C_3H_4 + OH \rightarrow C_2H_4 + CHO$, $C_3H_3 + H \rightarrow C_3H_4$ and $CHO + M \rightarrow CO + H + M$, respectively, are taken to dominate the consumption of these species, then the overall effects of steps 1, 5, and 6 of Table 1, for example, are as follows:

Reaction I is $C_{10}H_{16} + 2OH \rightarrow 2H + 3C_2H_4 + C_2H_2 + 2CO + H_2$.

Reaction II is $C_{10}H_{16} + O_2 + 2OH \rightarrow H + 3C_2H_4 + C_2H_2 + 2CO + H_2 + HO_2$.

Reaction III is $C_{10}H_{16} + 3OH \rightarrow H + 4C_2H_4 + 2CO + H_2O$.

Reactions I–III occur at the rates of steps 1, 5, and 6 of Table 1, respectively. None of these overall steps are net radical producers, and the likely most dominant one of the three during induction, step 6, which results in reaction III, exhibits a net consumption of two radicals for each OH attack on $C_{10}H_{16}$. The net radical removal by the fuel, thus, is the major source of the induction delay, contrary to the lighter fuels analyzed in previous publications.

These observations suggest a highly simplified approach to correlating ignition delay times. Approximate the $C_{10}H_{16}$ removal process during induction in Fig. 3 as being of first order with respect to $C_{10}H_{16}$ and controlled by the rate of oxidative pyrolysis given by step 5 of Table 1. Augment this rate by a factor of 10^4 to account for the much more rapid radical attack. The consequent e-folding time for the $C_{10}H_{16}$ concentration is $(10^4 k_5 [O_2])^{-1}$. Assume that 10 e-folding times are needed to reduce the $C_{10}H_{16}$ concentration to a value small enough compared with radical concentrations for the chain-branching thermal runaway of ignition to occur. The result, with the data in Table 1, is the ignition-time estimate given earlier in Eq. (1). The comparisons in Fig. 2 show this rough approximation to be remarkably good.

The success of this simplified approximation is largely fortuitous. It effectively focuses only on reaction II, ignoring reactions I and III. Reaction II, through its dependence on step 5 of Table 1, happens to have the right activation energy to fit the data. Reaction I would have the higher activation energy of reaction 1, and reaction III would effectively have a lower activation energy resulting mainly from the temperature dependence of the OH radical concentration in step 6, found[10] to be an appreciably weaker temperature dependence than the Arrhenius factor of step 5. The choice of reaction II, thus, is a compromise that appears to represent reasonably well the average effect of all steps. Pursuit of better-reasoned analyses of simplified descriptions is a worthwhile future activity.

Conclusions

A relatively short detailed mechanism is identified here that produces reasonable agreement with measured ignition times of JP-10. When ignition histories and possible reduced mechanisms are considered, a good theoretical correlation of experimental ignition delays is obtained. More work needs to be done to improve the basic description and also to simplify it more systematically for future use.

Acknowledgments

This work was supported by the Office of Naval Research through Contract N00014-99-1-0745. We thank S. L. Anderson, M. B. Colket, F. L. Dryer, R. K. Hanson, and W. Tsang for discussions.

References

[1] Li, S. C., and Williams, F. A., "Counterflow Heptane Flame Structure," *Proceedings of the Combustion Institute*, Vol. 28, 2001, pp. 1031–1038.

[2] Williams, F. A., Hanson, R. K., and Segal, C., "Fundamental Investigations of Pulse-Detonation Phenomena," JANNAF, Cocoa Beach, FL, 1999.

[3] Held, T. J., Marchese, A. J., and Dryer, F. L., "A Semi-Empirical Reaction Mechanism for n-Heptane Oxidation and Pyrolysis," *Combustion Science and Technology*, Vol. 123, Nos. 1–6, 1997, pp. 107–146.

[4] Szekely, G. A., Jr., and Faeth, G. M., "Effects of Envelope Flames on Drop Gasification Rates in Turbulent Diffusion Flames," *Combustion and Flame*, Vol. 49, Nos. 1–3, 1983, pp. 255–259.

[5] Takahashi, F., Dryer, F. L., and Williams, F. A., "Combustion Behavior of Free Boron Slurry Droplets," *Proceedings of the Combustion Institute*, Vol. 21, 1986, pp. 1983–1981.

[6] Wong, S.-C., and Lin, A.-C., "Microexplosion Mechanisms of Aluminum/Carbon Slurry Droplets," *Combustion and Flame*, Vol. 89, No. 1, 1992, pp. 64–76.

[7] Ryan, T. W., Schwab, S. T., and Harlowe, W. W., "Aluminum Alkyl Derivatives, Ignition and Combustion Enhancers for Supersonic Combustors," *Journal of Propulsion and Power*, Vol. 11, No. 1, 1995, pp. 1–24.

[8] Colket, M. B., III, and Spadaccini, L. J., "Scramjet Autoignition Study," *Journal of Propulsion and Power*, Vol. 17, No. 2, 2001, pp. 315–323.

[9] Davidson, D. F., Horning, D. C., Herbon, J. T., and Hanson, R. K., "Shock Tube Measurements of JP-10 Ignition," *Proceedings of the Combustion Institute*, Vol. 28, 2001, pp. 1687–1692.

[10] Varatharajan, B., and Williams, F. A., "Chemistry of Ethylene Ignition and Detonation, Part 1: Detailed Modeling and Experimental Comparison," *Journal of Propulsion and Power* (to be published); also AIAA Paper 2000-3475.

[11] Li, S. C., and Williams, F. A., "NO_x Formation in Two-Stage Methane–Air Flames," *Combustion and Flame*, Vol. 118, No. 3, 1999, pp. 399–414.

[12] Li, S. C., and Williams, F. A., "Reaction Mechanisms for Methane Ignition," *Journal of Engineering for Gas Turbines and Power* (to be published); also American Society of Mechanical Engineers Paper 2000-GT-0145.

[13] Li, S. C., and Williams, F. A., "Formation of NO_x, CH_4, and C_2 Species in Laminar Methanol Flames," *Proceedings of the Combustion Institute*, Vol. 27, 1998, pp. 485–493.

[14] Varatharajan, B., and Williams, F. A., “Chemical–Kinetic Descriptions of High-Temperature Ignition and Detonation of Acetylene–Oxygen-Diluent Systems,” *Combustion and Flame*, Vol. 124, No. 4, 2001, pp. 624–645.

[15] Waly, M. M. Y., Li, S. C., and Williams, F. A., “Structures of Non-sooting Counterflow Diluted Acetylene–Air Flames,” *Proceedings of the Combustion Institute*, Vol. 28, 2000, pp. 2005–2012.

[16] Waly, M. M. Y., Li, S. C., and Williams, F. A., “Experimental and Numerical Studies of Two-Stage Ethane–Air Flames,” *Journal of Engineering for Gas Turbines and Power*, Vol. 122, No. 4, 2000, pp. 651–658.

[17] Green, R. J., and Anderson, S. L., “Pyrolysis Chemistry of JP-10,”*Proceeding of the 13th ONR Propulsion Meeting*, ONR, Salt Lake City, UT, 2000, pp. 271–276.

[18] Douté, C., Delfau, J., and Vovelle, C., “Modeling of the Structure of a Premixed n-Decane Flame,” *Combustion Science and Technology*, Vol. 130, Nos. 1–6, 1997, pp. 269–313.

[19] Marchese, A. J., Dryer, F. L., and Nayagam, V., “Numerical Modeling of Isolated n-Alkane Droplet Flames: Initial Comparison with Ground and Space-Based Microgravity Experiments,” *Combustion and Flame*, Vol. 116, No. 3, 1999, pp. 432–459.

[20] Tsang, W., “Comparative-Rate Single-Pulse Shock Tube Studies on the Thermal Stability of Polyatomic Molecules,” *Shock Waves in Chemistry*, edited by A. Lifshitz, Marcel Decker, New York, 1981, pp. 59–129.

[21] Pitsch, H., “Entwicklug eines Programmpaketes zur Berechnung eindimensionaler Flammen am Beispeil einer Gegenstomdiffusionsflamme,” M.S. Thesis, Institut für Technische Mechanik, Rheinisch Westfälischen Technischen Hochschule Aachen, Aachen, Germany, Jan. 1993.

J. P. Gore
Associate Editor